Wideband Characterization of Backscatter Channels

Daniel Arnitz*, Ulrich Muehlmann**, and Klaus Witrisal*

* Signal Processing and Speech Communication Laboratory, Graz University of Technology, Austria
{daniel.arnitz, witrisal}@tugraz.at
** NXP Semiconductors, Gratkorn, Austria
ulrich.muehlmann@nxp.com

***Abstract*—The wireless channel of backscatter radio systems is a two-way pinhole channel, created by the concatenation of two standard wireless channels. Pinhole channels cause higher attenuation and deeper fades than common wireless channels.**

Passive ultra-high frequency radio-frequency identification (UHF RFID) is such a backscatter radio system, with the backscattering tag acting as pinhole. While the effects of this type of channel are well-known in terms of fading statistics, the impact of the pinhole channel on wideband parameters is unknown.

We present a method to calculate wideband backscatter channel parameters from the parameters of the constituent channels to and from the pinhole, with a focus on characteristics that are vital for narrowband and wideband ranging. The approximations are verified by simulations and by measurements in a UHF RFID warehouse portal.

I. Introduction

Pinhole channels are created by the concatenation of the channel from the transmitter to the pinhole and the channel from the pinhole to the receiver. In (semi-)passive ultra-high frequency radio-frequency identification (UHF RFID), a prime example for backscatter radio systems, the pinhole is formed by the backscattering tag, as illustrated in Fig. 1. The overall backscatter channel between transmitter (TX) and receiver (RX) at the reader is composed of the two individual channels to and from the tag. Both constituent channels are multipath radio channels. Pinhole (a.k.a. keyhole, dyadic, double-fading, or relay) channels are quite well-understood in terms of fading statistics for narrowband signals [1]–[4] and channel capacity for multi-input multi-output (MIMO) systems [5]–[7]. Even though channel capacity and fading statistics are fully sufficient to analyze the performance of communications, they are insufficient for the analysis of narrowband and wideband indoor localization systems (with the exception of receive-power based methods). We will thus concentrate on a more general description of the channel, the power-delay-profile (PDP), which is essentially the squared magnitude of the channel impulse response (CIR). The authors of [8] present an expression for the PDP of pinhole channels, but limited to orthogonal constituent channels. Moreover, no further parameterization of the pinhole-PDP is provided.

We present a closed-form expression for the PDP of typical indoor backscatter channels based on the PDPs of the constituent (point-to-point) channels, both for correlated and for uncorrelated point-to-point channels. We also present approximations for common wideband channel parameters, such as K-factor and root-mean-square (RMS) delay spread. These approximations are valid for exponential and non-exponential PDPs in line-of-sight (LOS) and non-line-of-sight (NLOS) scenarios, correlated and uncorrelated constituent channels, and also for predominantly deterministic channels, as shown below.

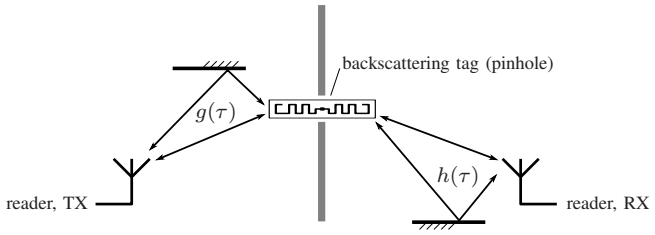

Fig. 1. Illustration of the pinhole effect in (semi)passive UHF RFID systems. In reality, each channel is composed of up to thousands of relevant paths.

The paper is organized as follows: Section II introduces the notation, defines the channel (model) parameters, and discusses their influence on ranging. The following Section III contains closed-form expressions for the channel parameters of the backscatter channel based on the point-to-point channel parameters. These expressions are verified in Section IV using simulated and measured indoor wireless channels.

II. Basics and Background Information

A. Wireless Channels

Like any linear system, wireless channels can be represented by their impulse response, the CIR. Wireless CIRs are typically modeled in a random fashion in order to account for the typically unknown and time-variant environment. Similar to the power spectral density for random signals, the power delay profile (PDP) is used to describe the frequency-selective random channel. The PDP (a.k.a. delay power spectrum or multipath intensity profile) is essentially defined as the autocorrelation function of the CIR, and can be estimated by averaging squared CIRs (averaged power delay profile, APDP). More details along with necessary requirements and limitations can for example be found in [9], [10] or textbooks such as [7], [11].

The first arriving component of a wireless CIR corresponds to the direct (line-of-sight, LOS) path and all following components to indirect (reflected, non-line-of-sight, NLOS) paths.

In Fig. 1 the CIR of the channel from the transmitter (TX) to the tag, for example, is denoted by $g(\tau)$, where τ is the propagation delay. For notational simplicity, we will assume that the LOS component is at a delay of $\tau_{\text{LOS}} = 0$ for all channels. This has no influence on the results in this paper, as all analyzed channel parameters are shift-invariant[1]. Also note that all CIRs are zero for $\tau < \tau_{\text{LOS}}$ and thus $\tau < 0$, because the LOS is per definition the first nonzero component.

From the PDP, denoted by $S(\tau)$ below, we can calculate several measures that characterize the wireless channel. The power ratio of the direct path to all indirect paths is of vital importance for localization, as it quantifies the influence of the direct path on the CIR. This ratio is provided by the K-factor w.r.t. the LOS path,

$$K_{\text{LOS}} = \frac{P_{\text{LOS}}}{P_{\text{NLOS}}} = \frac{P_{\text{LOS}}}{\int_0^\infty S(\tau)d\tau - P_{\text{LOS}}}, \tag{1}$$

where P_{LOS} and P_{NLOS} are line-of-sight and non-line-of-sight power, respectively. Note that this is not necessarily identical to the definition of the Ricean K-factor, which uses the strongest path instead of the direct path. A second measure relevant for localization is the root-mean-square (RMS) delay spread,

$$\tau_{\text{RMS}} = \sqrt{\frac{\int_0^\infty \tau^2 S(\tau)d\tau}{\int_0^\infty S(\tau)d\tau} - \left(\frac{\int_0^\infty \tau S(\tau)d\tau}{\int_0^\infty S(\tau)d\tau}\right)^2}, \tag{2}$$

which specifies the decay of the CIR over delay.

Although these channel parameters are defined based on the PDP (a fully deterministic function), they can also be calculated from each individual squared CIR, which is often called "instantaneous PDP". Note though, that the squared CIR is a random process, hence all parameters derived from instantaneous PDPs are random variables.

B. Effects of Multipath Propagation on Ranging Errors

The impact of multipath propagation on RF-based ranging (i.e., distance estimation) systems depends on the signal bandwidth and the properties of the channel. Limiting the bandwith leads to a smoothed CIR due to the uncertainty relation between time- and frequency-domain representations. For narrowband systems, the entire CIR collapses to a single complex gain factor. If the direct path is dominant in the CIR, i.e., the instantaneous K_{LOS} is large, the direct path is also dominant in the complex gain factor, and narrowband ranging will give accurate results. For low K_{LOS}, the gain factor is mainly determined by indirect and thus purely random paths. As a direct consequence, narrowband distance estimates will have a high standard deviation. Moreover, depending on τ_{RMS} and the shape of the PDP, the dominant NLOS results in a bias of the gain factor towards indirect paths, and thus also in a biased distance estimate. Similar considerations apply to all systems that are unable to isolate the LOS component. The PDP, along with shape parameters such as K_{LOS} and τ_{RMS}, can be used to calculate the expected distance errors of such ranging systems (bias and std. deviation). However, if the LOS component is correctly identified and extracted, the shape of the PDP looses its influence on the ranging error. This usually requires a large signal bandwidth, though.

[1]The K-factor is a simple power ratio and does thus not depend on the delay axis at all. The RMS delay spread is a central moment, hence the average time shift is irrelevant.

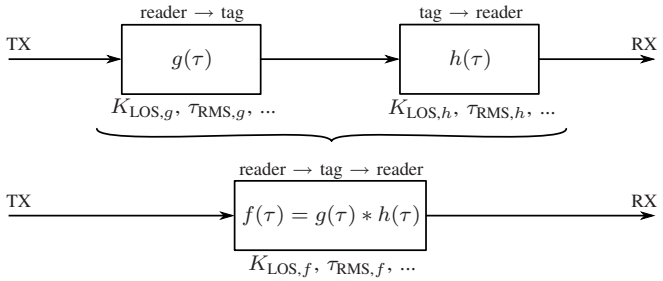

Fig. 2. Combination of individual channels reader→tag (downlink) and tag→reader (uplink) to the backscatter channel reader→tag→reader.

Passive UHF RFID is one of the most challenging scenarios for backscatter-based localization. The system is typically used indoors and in industrial or industrial-like environments [12]–[14], with massive reflections close to the backscattering tag. These features, along with the pinhole properties of the channel, create a severe multipath environment, where the direct path is rarely dominant and very large bandwidths are required to properly resolve the closely spaced components [12], [13]. Conventional wideband approaches such as multi-carrier or frequency-modulated continuous-wave radar (e.g., [15], [16]) suffer from biased and high-variance estimates in such environments [12], [17]. Ultra-wideband methods such as [18] are able to correctly identify the LOS path, but suffer from the massive channel attenuation due to the backscatter nature and the low signal-to-self-interference ratios, cf. [12].

C. Pinhole and Backscatter Wireless Channels

As mentioned in the introduction and illustrated in Figs. 1 and 2, the backscatter channel is the concatenation of two wireless channels and as such always a pinhole channel. In the terminology of RFID, the channel from the reader to the tag is called "downlink channel", while the channel from the tag to the reader is called "uplink channel", cf. [19]. Up- and downlink channel are identical for monostatic setups, where the reader uses only one antenna for simultaneous transmission and reception. For bistatic reader setups, on the other hand, they can be (almost) independent, since TX- and RX-antenna are spatially distinct, cf. [20].

The individual channels to and from the pinhole, represented by their respective CIRs $g(\tau)$ and $h(\tau)$, each have their own set of channel parameters (K_{LOS}, τ_{RMS}, ...). It is straightforward to see from Fig. 2 that the backscatter CIR $f(\tau)$ can be calculated by the convolution of $g(\tau)$ and $h(\tau)$. The connection between the channel parameters of the backscatter channel and their counterparts of the individual channels, on the other hand, is less obvious. Apart from the mathematical point of

view, which can be found below, we can make some basic observations regarding the backscatter channel. For this, we refer to a channel with low K_{LOS} and high τ_{RMS} as a "bad" channel, while a channel with high K_{LOS} and/or low τ_{RMS} is "better" in comparison, i.e., a "good" channel.

- The combined channel is always worse than both individual channels. This follows directly from the convolution, which results in a longer channel impulse response and dispersed peaks (also affecting the LOS peak).
- Correlation between up- and downlink channel has an adverse effect on the backscatter channel, because coherent combining of the random NLOS-parts increases the NLOS energy[2].
- The statistics of the worse channel dominate the statistics of the backscatter channel. Hence in bistatic setups, both reader antennas need to have a clear line-of-sight to the tag in order to obtain a good backscatter channel. Also this fact can be inferred from the convolution operation: The convolution of an ideal CIR w.r.t. ranging (a dirac) with any dispersive CIR, for example, results in the dispersive (i.e, bad) one for the overall channel.

III. Approximation Formulas

A. Power-Delay-Profile

It has been shown in [8] that the PDP of a pinhole channel can be obtained by a convolution of the PDPs of up- and downlink channel, provided that these channels are uncorrelated.

By separating the power-delay-profiles of the channels to and from the tag, $S_g(\tau)$ and $S_h(\tau)$, into LOS and NLOS parts

$$S_g(\tau) = S_{g,\text{LOS}} \cdot \delta(\tau) + S_{g,\text{NLOS}}(\tau) \cdot \sigma(\tau) \tag{3}$$

$$S_h(\tau) = S_{h,\text{LOS}} \cdot \delta(\tau) + S_{h,\text{NLOS}}(\tau) \cdot \sigma(\tau) \tag{4}$$

the convolution of the PDPs can be written as

$$\begin{aligned} S_{f,\text{uncorr}}(\tau) = S_g(\tau) * S_h(\tau) = S_{g,\text{LOS}} \cdot S_{h,\text{LOS}} \cdot \delta(\tau) \\ + \sigma(\tau) \cdot [S_{g,\text{LOS}} \cdot S_{h,\text{NLOS}}(\tau) + S_{h,\text{LOS}} \cdot S_{g,\text{NLOS}}(\tau) \\ + S_{g,\text{NLOS}}(\tau) * S_{h,\text{NLOS}}(\tau)]. \end{aligned} \tag{5}$$

where $*$ denotes the convolution, $\delta(\tau)$ is the Dirac delta, and $\sigma(\tau)$ is the step function

$$\sigma(\tau) = \begin{cases} 1 & \tau > 0 \\ 0 & \text{otherwise} \end{cases}. \tag{6}$$

$S_{f,\text{uncorr}}(\tau)$ is the backscatter PDP for uncorrelated constituent channels, cf. [8], [21]. Splitting this PDP into LOS and NLOS parts, we obtain

$$S_{f,\text{LOS}} = S_{g,\text{LOS}} \cdot S_{h,\text{LOS}} \tag{7}$$

and

$$\begin{aligned} S_{f,\text{NLOS,uncorr}}(\tau) = S_{g,\text{LOS}} \cdot S_{h,\text{NLOS}}(\tau) + S_{h,\text{LOS}} \cdot S_{g,\text{NLOS}}(\tau) \\ + S_{g,\text{NLOS}}(\tau) * S_{h,\text{NLOS}}(\tau). \end{aligned} \tag{8}$$

[2]An effect that can also be seen for the variance of two additive random variables.

Coherent combining of the stochastic NLOS part in case of fully correlated up- and downlink channels doubles the NLOS power without changing the shape of the NLOS part [21], hence

$$S_{f,\text{NLOS,corr}}(\tau) = 2 \cdot S_{f,\text{NLOS,uncorr}}(\tau). \tag{9}$$

Full correlation between the constituent channels also implies that their K-factors and RMS delay spreads are identical [21], i.e., $\tau_{\text{RMS},g} = \tau_{\text{RMS},h}$ and $K_{\text{LOS},g} = K_{\text{LOS},h}$.

Passive UHF RFID is typically used indoors, where the rich scattering leads to exponential PDPs (e.g., [22], [23]). For the following derivations we thus assume exponential short-range indoor PDPs for the two individual channels g and h,

$$S_g(\tau) = \begin{cases} 0 & \tau < 0 \\ \rho_g^2 & \tau = 0 \\ \Pi_g \mathrm{e}^{-\gamma_g \tau} & \tau > 0 \end{cases} \quad \text{and} \tag{10}$$

$$S_h(\tau) = \begin{cases} 0 & \tau < 0 \\ \rho_h^2 & \tau = 0 \\ \Pi_h \mathrm{e}^{-\gamma_h \tau} & \tau > 0 \end{cases}, \tag{11}$$

where ρ_g^2 and ρ_h^2 are the LOS power levels of channels g and h, respectively, Π_g and Π_h are the NLOS power densities, and γ_g and γ_h are the decay constants of the channels, cf. [24].

Using these definitions, we calculate the closed-form PDP of short-range indoor backscatter channels. The LOS component of this PDP is

$$S_{f,\text{LOS}} = \rho_g^2 \rho_h^2, \tag{12}$$

and the NLOS part for uncorrelated channels is

$$\begin{aligned} S_{f,\text{NLOS,uncorr}}(\tau) = \rho_g^2 \Pi_h \mathrm{e}^{-\gamma_h \tau} + \rho_h^2 \Pi_g \mathrm{e}^{-\gamma_g \tau} \\ + \frac{\Pi_g \Pi_h}{\gamma_g - \gamma_h} \left(\mathrm{e}^{-\gamma_h \tau} - \mathrm{e}^{-\gamma_g \tau} \right). \end{aligned} \tag{13}$$

The NLOS-part is multiplied by a factor of two for correlated constituent channels, see (9).

From this we will calculate K-factor and the RMS delay spread of the combined backscatter channel. Formulas linking ρ, Π, and γ with K_{LOS} and τ_{RMS} for the exponential PDPs are readily provided by [24],

$$\Pi = \frac{P_0}{K_{\text{LOS}} + 1} \gamma, \tag{14}$$

$$\gamma = \frac{1}{\tau_{\text{RMS}}} \frac{\sqrt{2K_{\text{LOS}} + 1}}{K_{\text{LOS}} + 1}, \tag{15}$$

$$\rho^2 = P_0 \frac{K_{\text{LOS}}}{K_{\text{LOS}} + 1}, \tag{16}$$

where the overall power $P_{\text{LOS}} + P_{\text{NLOS}}$ is denoted by P_0.

B. K-Factor w.r.t. the Line-of-Sight Component

The K-factor can be directly calculated from (1) by inserting (12) and (13). Substituting (14)–(16) then leads to

$$\begin{aligned} K_{\text{LOS},f} &= \frac{S_{f,\text{LOS}}}{\int_0^\infty S_{f,\text{NLOS}}(\tau)\, d\tau} \\ &= \left(1 - \frac{\alpha_K}{2}\right) \cdot \frac{K_{\text{LOS},g} \cdot K_{\text{LOS},h}}{1 + K_{\text{LOS},g} + K_{\text{LOS},h}}. \end{aligned} \tag{17}$$

where the parameter $0 \leq \alpha_K \leq 1$ represents correlation between the channels g and h. Due to the doubling of the NLOS energy for correlated up- and downlink, cf. (9), we obtain

$$\alpha_K = \begin{cases} 0 & g(\tau) \text{ and } h(\tau) \text{ uncorr.} \\ 1 & g(\tau) \text{ and } h(\tau) \text{ fully corr.} \end{cases}. \tag{18}$$

C. RMS Delay Spread

The RMS delay spread is calculated from the backscatter PDP via

$$\tau_{\text{RMS},f} = \sqrt{\frac{\int_0^\infty \tau^2 S_{f,\text{NLOS}}(\tau)d\tau}{S_{f,\text{LOS}} + \int_0^\infty S_{f,\text{NLOS}}(\tau)d\tau} - \tau_{\text{AVG},f}^2}, \tag{19}$$

cf. (2), where

$$\tau_{\text{AVG},f} = \frac{\int_0^\infty \tau S_{f,\text{NLOS}}(\tau)d\tau}{S_{f,\text{LOS}} + \int_0^\infty S_{f,\text{NLOS}}(\tau)d\tau} \tag{20}$$

is the average delay. By solving these equations for (12) and (13) we obtain the RMS delay spread for uncorrelated channels,

$$\tau_{\text{RMS},f,\text{uncorr.}} = \sqrt{\tau_{\text{RMS},g}^2 + \tau_{\text{RMS},h}^2}, \tag{21}$$

with (14)–(16). The same result can also be reached by using a similarity to statistics: Just like the PDPs of uncorrelated constituent channels the density functions of two added uncorrelated random variables are convolved and the variances add up. From this observation is it straightforward to see that (21) holds for arbitrary types of PDPs.

For correlated channels though, things are more complicated. Looking at the structure of (19) and (20), the doubling of NLOS-power for correlated channels, cf. (9), will lead to an imbalance in the denominators. As a consequence, the ratio between LOS- and NLOS-power—and thus K_{LOS}—has an influence on the result. Following the same derivation as for (21) with doubled NLOS-power we obtain

$$\begin{aligned} \tau_{\text{RMS},f,\text{corr.}} &= \sqrt{\frac{2\int_0^\infty \tau^2 S_{f,\text{NLOS}}(\tau)d\tau}{S_{f,\text{LOS}} + 2\int_0^\infty S_{f,\text{NLOS}}(\tau)d\tau} - \ldots} \\ &= \tau_{\text{RMS},g}\sqrt{2 + 2\alpha_\tau} \end{aligned} \tag{22}$$

for fully correlated channels and with $\tau_{\text{RMS},g} = \tau_{\text{RMS},h}$ (full correlation). The parameter α_τ here represents the correlation and is also obtained from the above calculations,

$$\begin{aligned} \alpha_\tau &= \frac{K_{\text{LOS},g}^2 \cdot \left(K_{\text{LOS},g}^2 \cdot (2K_{\text{LOS},g} + 5) - 2\right)}{(1 + 2K_{\text{LOS},g}) \cdot (K_{\text{LOS},g} \cdot (K_{\text{LOS},g} + 4) + 2)^2} \\ &\approx \frac{K_{\text{LOS},g}}{10 + K_{\text{LOS},g}} \end{aligned} \tag{23}$$

with $K_{\text{LOS},g} = K_{\text{LOS},h}$ due to the full correlation.

While it can again be shown that (22) holds for arbitrary PDPs [21], (23) is derived specifically for exponential ones. However, the PDPs of all wireless channels have a similar shape due to the fact that they decay for increasing delay. Hence (23) is a suitable approximation even for channels with non-exponential PDPs, as can be seen from the measurement results in Section IV-B. Finally, α_τ vanishes for low K-factors, hence correlation between the constituent channels can be ignored if the NLOS component is dominant on the backscatter link, and the result again becomes independent of the type of PDP.

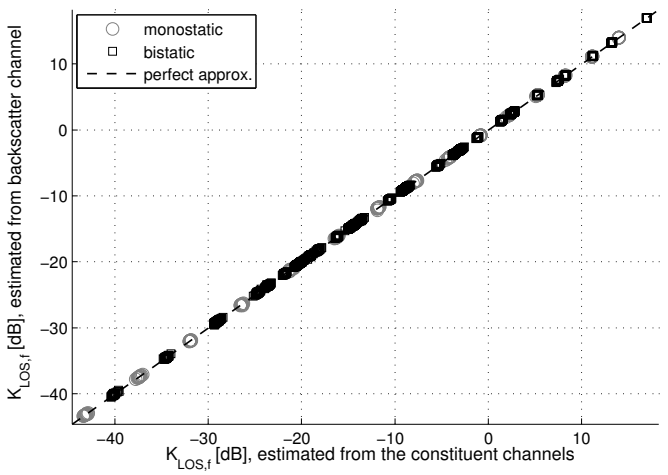

Fig. 3. Approximation of the backscatter K-factor w.r.t. LOS for simulated exponential power-delay-profiles. Estimates are based on averaged PDPs.

IV. Validation Based on Simulations and Measurements

The above approximations are tested with simulated and measured channel impulse responses in this section. To this end, we compare the approximations based on parameters estimated from the PDPs of the constituent channels, $S_g(\tau)$ and $S_h(\tau)$, to parameters directly estimated from the backscatter PDP (channel f). Both estimates match in the ideal case, resulting in a $45\,^\circ$ line in the plots.

The simulated channels with known expected values for all parameters are used to verify the estimates in controlled environments, while the validation with measured channel impulse responses ensures robustness in realistic propagation environments. The measurements cover exponential and non-exponential PDPs, LOS and NLOS scenarios, as well as channels where the LOS component is massively influenced by spatially close reflections.

A. Simulated Exponential Power-Delay-Profiles

The simulated random CIRs have been generated by the smallscale model of the PARIS framework [25], [26], which implements a sampled version of the exponential PDP in [24] and is thus fully defined by K_{LOS} and τ_{RMS}. K-factor and RMS delay spread in the simulations were swept from -20 to 20 dB and from 3 through 50 ns, respectively, for the average PDP of both constituent channels. This should cover most typical indoor scenarios, cf. [12], [13], [27], [28]. An ensemble of 100 instantaneous PDPs is averaged for each combination of $K_{\text{LOS},g}$, $K_{\text{LOS},h}$, $\tau_{\text{RMS},g}$, and $\tau_{\text{RMS},h}$. Some residual "noise" can thus be expected in the estimates.

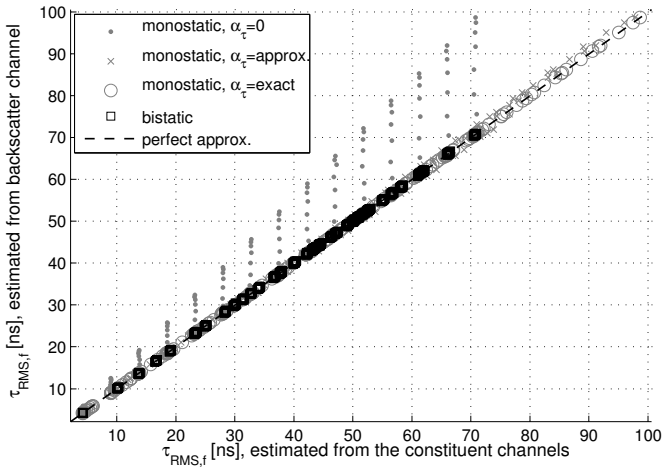

Fig. 4. Approximation of the backscatter RMS delay spread for simulated exponential power-delay-profiles. Estimates are based on averaged PDPs.

The results of this Monte-Carlo-simulation are shown in Fig. 3 for the K-Factor and Fig. 4 for the RMS delay spread. The K-factor calculated from the constituent channel parameters using (17) matches the K-factor of the combined pinhole channel throughout the simulated range, both for the monostatic (fully correlated) and the bistatic (uncorrelated) setup. The RMS delay spreads for the bistatic setup and the exact monostatic approximation according to (22) and (23) show a perfect match, too. Using the simplified formula for α_τ leads to a nonperfect but nontheless quite good approximation of the RMS delay spread for the monostatic case. If correlation is completely ignored though ($\alpha_\tau = 0$), the approximation is increasingly off for $K_{\mathrm{LOS},g} = K_{\mathrm{LOS},h} > -3\,\mathrm{dB}$.

B. Measured Power-Delay-Profiles

The used measurements were taken in a UHF RFID warehouse portal with metal backplanes, in an industrial environment, and with directive reader antennas, see [12], [13]. The tag-antennas were mounted on a pallet containing liquids and metal. This creates an intense and very variable multipath environment with strong deterministic reflections. A photograph of this setup can be found in Fig. 5; details are presented in [12] and [13].

The channels inside the portal have a multipath decay according to a power-law, while the channels outside the portal feature an exponential decay [12]. The direct path between transmitter, tag, and receiver (backscatter channel) is blocked by the pallet for $43\,\%$ of the measured channels. The measurements thus not only cover "typical" exponential PDPs and LOS scenarios, but also differently shaped delay-profiles and NLOS scenarios. Mounting the tag-antennas directly on the pallet also causes indirect (NLOS) paths to be part of the LOS component due to the necessarily limited measurement bandwidth. Moreover, multiple deterministic reflections inside the gate cause correlation within the CIRs of up- and downlink. This violates one of the basic assumptions underlying the theory behind the approximation formulas given in this paper,

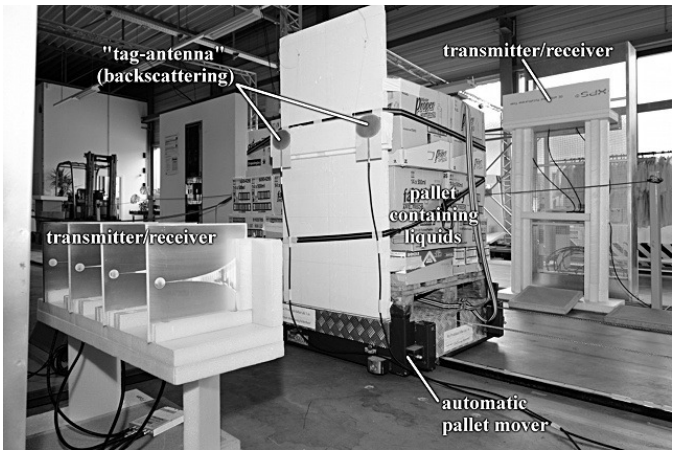

Fig. 5. Photograph of the warehouse gate with metal backplanes (directly behind the transmitter/receiver arrays) and the pallet with packed liquids/metals.

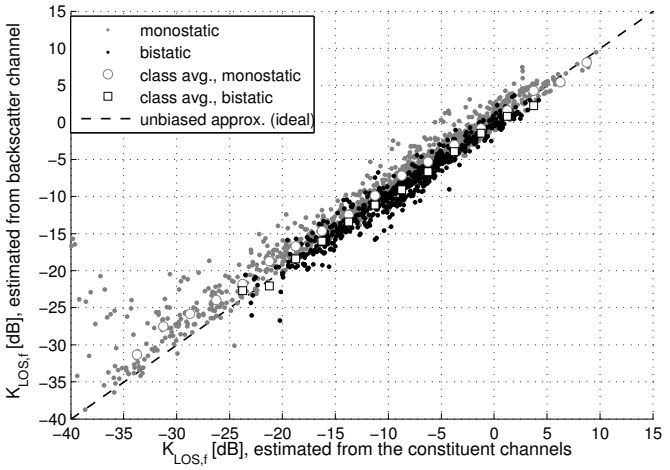

Fig. 6. Approximation of the backscatter K-factor w.r.t. LOS for measured power-delay-profiles (UHF RFID warehouse portal, metal portal, liquids/metal pallet). Estimates are based on individual (instantaneous) power-delay-profiles; averages are shown for comparison.

cf. [21]. The portal scenario is thus not only a challenging example for backscatter-based localization, but also for the approximation methods presented in this paper.

The results for the measured channels can be found in Figs. 6 and 7, respectively. Note that the noise level in these estimates is considerably higher than for the simulations in Figs. 3 and 4. This is because the simulated PDPs are averaged before estimating $K_{\mathrm{LOS},f}$ and $\tau_{\mathrm{RMS},f}$, while the measured parameters are calculated from individual (instantaneous) PDPs in order to show that the above equations can also be used as estimators for instantaneous PDPs. Averages are shown in the plots for comparison.

The backscatter channel parameters can obviously be predicted quite well from the individual ones. This includes the area inside the portal, where the PDP follows a power-law, and the area outside the portal, which features an exponential PDP, cf. [12]. The slight bias in $K_{\mathrm{LOS},f}$ for the monostatic

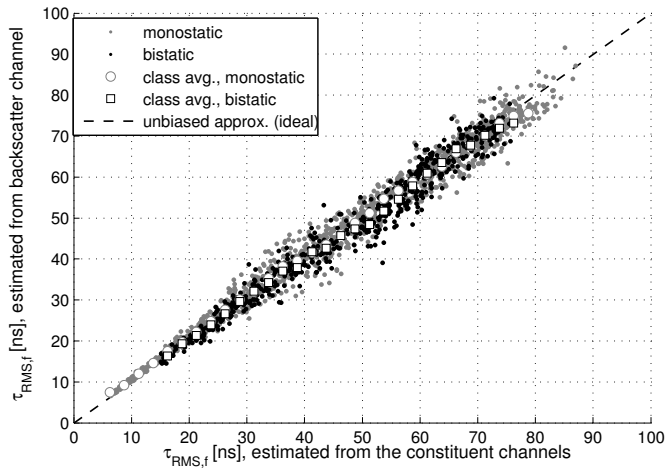

Fig. 7. Approximation of the backscatter RMS delay spread for measured power-delay-profiles (UHF RFID warehouse portal, metal portal, liquids/metal pallet). Estimates are based on individual (instantaneous) power-delay-profiles and use the simplified formula for α_τ in (23). Averages are shown for comparison.

setup is caused by reflections that could not be isolated from the LOS component with the given bandwidth. This leads to $\alpha_K < 1$ even though the constituent channels are fully correlated, cf. [21]. Naturally, this effect increases for weaker LOS, i.e., lower K_{LOS}. The outliers for very low K-factors in Fig. 6 are caused by false-positives in the LOS detection for the backscatter channel due to the weak LOS. For these points, the LOS component of the backscatter channel is close to or below the noisefloor of the measurements and cannot be detected reliably any more. The estimated K-factor then depends on which component the LOS-detection locks onto, but is always larger than the true $K_{\mathrm{LOS},f}$, explaining why all outliers are above the $45\,^\circ$ line.

V. Conclusion

Backscatter-based localization systems operate on the combined backscatter channel and thus have to deal with its pinhole nature. Detailed information regarding the backscatter channel is crucial to the analyses of such systems, yet the vast majority of characterizations and measurements are performed for point-to-point wireless channels, e.g., [12], [13], [28]–[30].

We presented a method to combine wideband parameters of wireless indoor radio channels to the parameters of the backscatter channel. Expressions for the K-factor w.r.t. the LOS path and the RMS delay spread of the backscatter channel based on the individual channels' parameters are given and validated using simulated and measured wireless indoor channel impulse responses. It is shown that these approximations are applicable and useful even in critical environments, where several of the theoretical assumptions do not hold.

The approximations can for example be used to estimate the performance of backscatter indoor localization systems based on point-to-point measurements of the channel. Although they are derived for the average PDP, they can be readily applied to squared CIRs, as shown in Figs. 6 and 7.

VI. Acknowledgments

The authors wish to thank the anonymous reviewers whose comments helped to substantially improve this contribution.

This work was funded by NXP Semiconductors, Gratkorn, Austria, and the Austrian Research Promotion Agency (FFG) under the grant number 818072.

References

[1] J. D. Griffin and G. D. Durgin, "Gains for RF tags using multiple antennas," *IEEE Trans. Antennas Propag.*, vol. 56, no. 2, pp. 563–570, 2008.

[2] T. Taniguchi, Y. Karasawa, and M. Tsuruta, "An analysis method of double fading MIMO channels including LOS environments," in *Proc. IEEE 19th Int. Symp. Personal, Indoor and Mobile Radio Communications PIMRC 2008*, 2008, pp. 1–5.

[3] J. D. Griffin and G. D. Durgin, "Link envelope correlation in the backscatter channel," *IEEE Commun. Lett.*, vol. 11, no. 9, pp. 735–737, 2007.

[4] D. Kim, M. A. Ingram, and J. Smith, W. W., "Measurements of small-scale fading and path loss for long range RF tags," *IEEE Trans. Antennas Propag.*, vol. 51, no. 8, pp. 1740–1749, 2003.

[5] P. L. Kafle, A. Intarapanich, A. B. Sesay, J. McRory, and R. J. Davies, "Spatial correlation and capacity measurements for wideband MIMO channels in indoor office environment," *IEEE Trans. Wireless Commun.*, vol. 7, no. 5, pp. 1560–1571, 2008.

[6] P. Almers, F. Tufvesson, and A. F. Molisch, "Keyhole effect in MIMO wireless channels: Measurements and theory," *IEEE Trans. Wireless Commun.*, vol. 5, no. 12, pp. 3596–3604, 2006.

[7] A. Paulraj, R. Nabar, and D. Gore, *Introduction to Space-Time Wireless Communications*. Cambridge University Press, 2003, ISBN-13: 9-780521826150.

[8] X. Yin, Y. Zhou, and F. Liu, "A generic wideband channel model for keyhole propagation scenarios and experimental evaluation," in *Proc. Fourth Int. Conf. Communications and Networking in China ChinaCOM 2009*, 2009, pp. 1–5.

[9] R. Kattenbach, "Statistical modeling of small-scale fading in directional radio channels," *IEEE J. Sel. Areas Commun.*, vol. 20, no. 3, pp. 584–592, 2002.

[10] P. Bello, "Characterization of randomly time-variant linear channels," *IEEE Transactions on Communications Systems*, vol. 11, no. 4, pp. 360–393, 1963.

[11] A. Molisch, *Wireless Communications*. John Wiley & Sons, 2005, ISBN-13: 978-0470848876.

[12] D. Arnitz, U. Muehlmann, and K. Witrisal, "Wideband characterization and modeling of UHF RFID channels for ranging and positioning," submitted to IEEE Trans. Antennas Propag.

[13] D. Arnitz, G. Adamiuk, U. Muehlmann, and K. Witrisal, "UWB channel sounding for ranging and positioning in passive UHF RFID," in *11th COST2100 MCM*, Aalborg, Denmark, Jun. 2010. [Online]. Available: http://www.spsc.tugraz.at/people/daniel-arnitz/ArnitzCOSTMCM10.pdf

[14] U. Muehlmann, G. Manzi, G. Wiednig, and M. Buchmann, "Modeling and performance characterization of UHF RFID portal applications," *IEEE Trans. Microw. Theory Tech.*, vol. 57, no. 7, pp. 1700–1706, 2009.

[15] S. Kunkel, M.-S. Huang, R. Bieber, and M. Vossiek, "SAR-like localization of RFID tags for non-uniform trajectory," in *Proc. European Wireless Technology Conf. (EuWIT)*, 2010, pp. 281–284.

[16] D. Arnitz, U. Muehlmann, and K. Witrisal, "Multi-frequency continuous-wave radar approach to ranging in passive UHF RFID," *IEEE Trans. Microw. Theory Tech.*, vol. 57, no. 5, pp. 1398–1405, Jul. 2009.

[17] G. Li, D. Arnitz, R. Ebelt, U. Muehlmann, K. Witrisal, and M. Vossiek, "Bandwidth dependence of CW ranging to UHF RFID tags in severe multipath environments," in *Proc. IEEE Int RFID Conf*, Orlando, Florida, Apr. 2011.

[18] D. Arnitz, U. Muehlmann, and K. Witrisal, "UWB ranging in passive UHF RFID: Proof of concept," *IET Electron. Letters*, vol. 46, no. 20, pp. 1401–1402, Sep. 2010.

[19] K. Finkenzeller, *RFID Handbook: Fundamentals and Applications in Contactless Smart Cards and Identification*, 2nd ed. Wiley & Sons, 2003, ISBN-13: 978-0470844021.

[20] J. D. Griffin and G. D. Durgin, "Complete link budgets for backscatter-radio and RFID systems," *IEEE Antennas Propag. Mag.*, vol. 51, no. 2, pp. 11–25, 2009.
[21] D. Arnitz, U. Muehlmann, and K. Witrisal, "Wideband characterization of backscatter channels: Derivations and theoretical background," submitted to IEEE Trans. Antennas Propag.
[22] L. J. Greenstein, S. S. Ghassemzadeh, S.-C. Hong, and V. Tarokh, "Comparison study of UWB indoor channel models," *IEEE Trans. Wireless Commun.*, vol. 6, no. 1, pp. 128–135, 2007.
[23] D. Cassioli, M. Z. Win, and A. F. Molisch, "The ultra-wide bandwidth indoor channel: from statistical model to simulations," *IEEE J. Sel. Areas Commun.*, vol. 20, no. 6, pp. 1247–1257, 2002.
[24] K. Witrisal, Y.-H. Kim, and R. Prasad, "A new method to measure parameters of frequency-selective radio channels using power measurements," *IEEE Trans. Commun.*, vol. 49, no. 10, pp. 1788–1800, Oct. 2001.
[25] The PARIS Simulation Framework. Graz University of Technology / NXP Semiconductors. Open-Source (GNU GPL v3). [Online]. Available: http://tinyurl.com/paris-osf/
[26] D. Arnitz, U. Muehlmann, T. Gigl, and K. Witrisal, "Wideband system-level simulator for passive UHF RFID," in *Proc. IEEE Int. Conf. on RFID*, Orlando, Florida, Apr. 2009.
[27] D. Arnitz, U. Muehlmann, and K. Witrisal, "Wideband characterization of UHF RFID channels for ranging and positioning," Poster at IEEE Int. Conf. on RFID, Apr. 2010. [Online]. Available: http://www.spsc.tugraz.at/people/daniel-arnitz/ArnitzRFID10.zip
[28] M. K. Awad, K. T. Wong, and Z.-b. Li, "An integrated overview of the open literature's empirical data on the indoor radiowave channel's delay properties," *IEEE Trans. Antennas Propag.*, vol. 56, no. 5, pp. 1451–1468, 2008.
[29] J. Karedal, S. Wyne, P. Almers, F. Tufvesson, and A. F. Molisch, "A measurement-based statistical model for industrial ultra-wideband channels," *IEEE Trans. Wireless Commun.*, vol. 6, no. 8, pp. 3028–3037, 2007.
[30] M. S. Varela and M. G. Sanchez, "RMS delay and coherence bandwidth measurements in indoor radio channels in the UHF band," *IEEE Trans. Veh. Technol.*, vol. 50, no. 2, pp. 515–525, 2001.